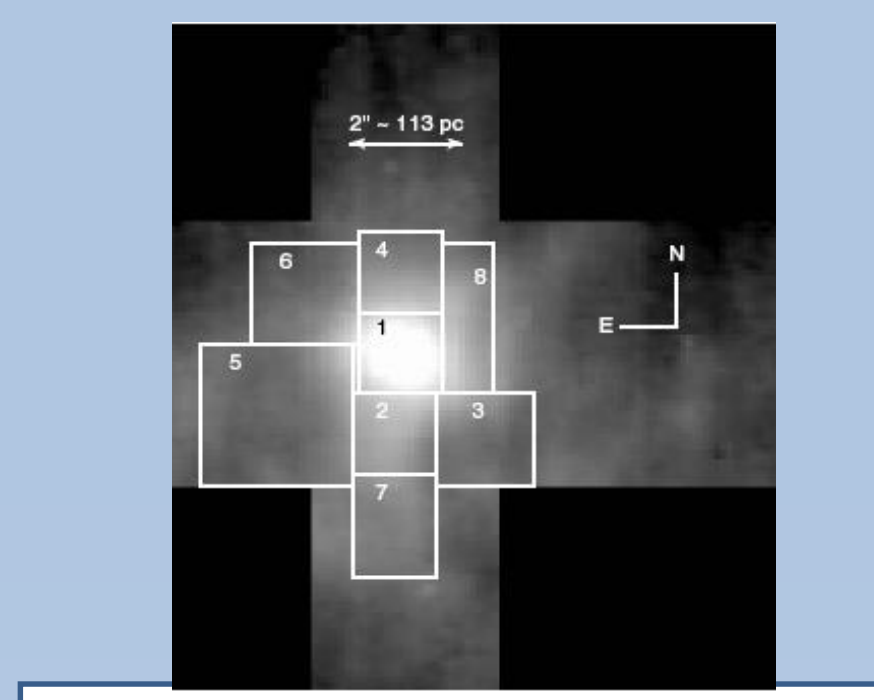
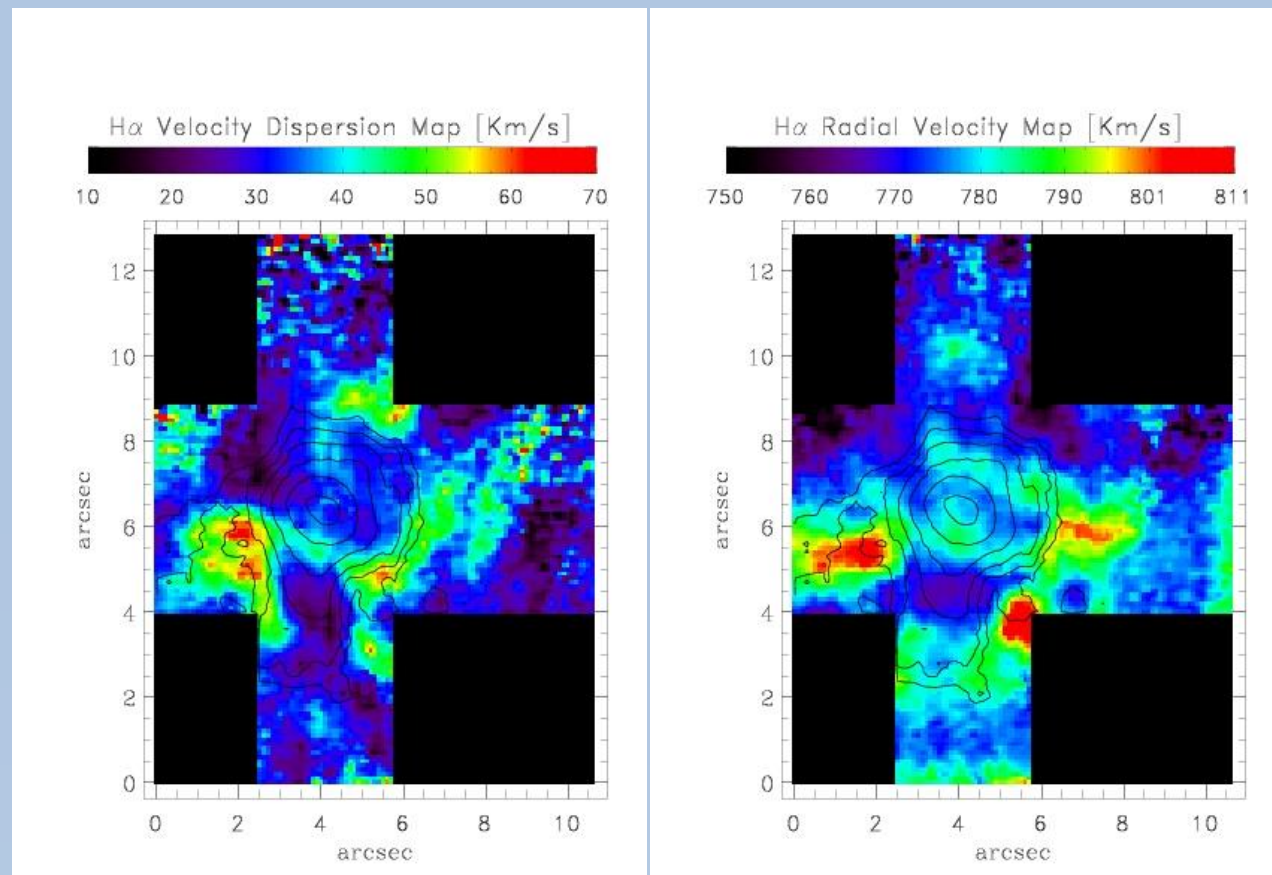


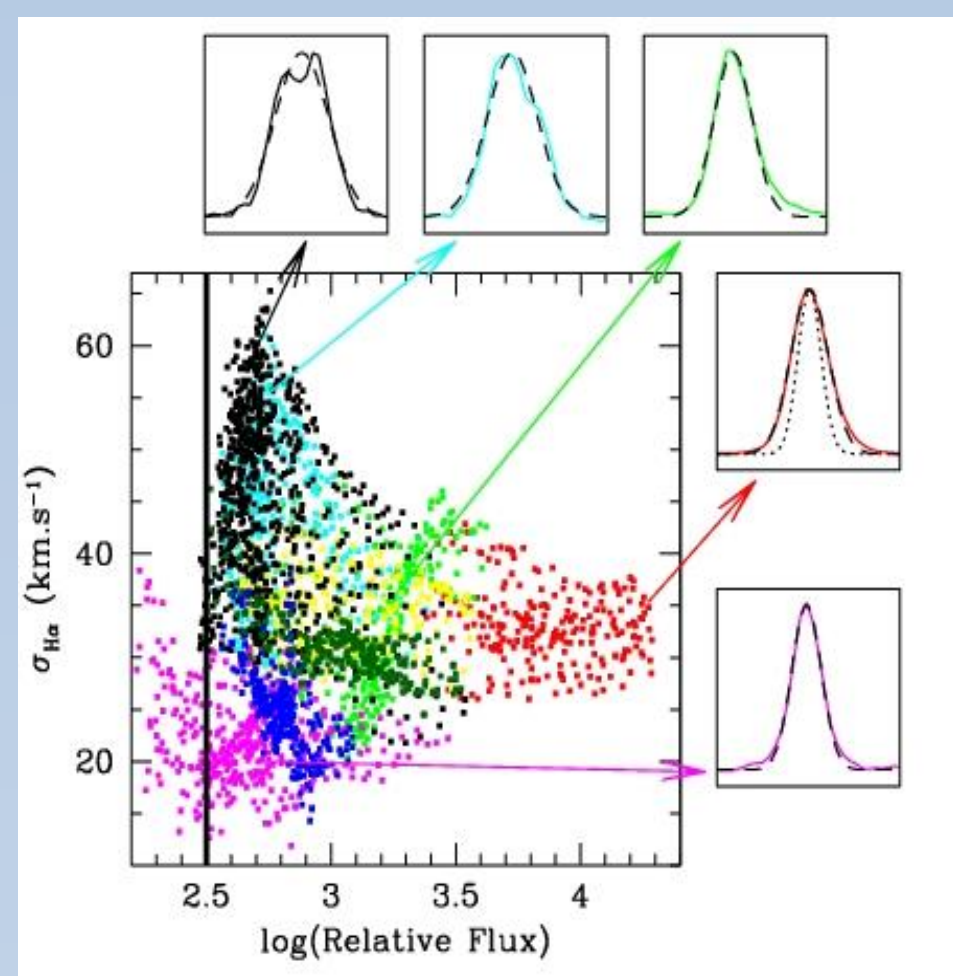
THE INTERNAL KINEMATICS OF II ZW 40



From optical GEMINI-GMOS/IFU, we derived the H α emission map. Eight individual regions were chosen to dissect the kinematics of the central starburst in II Zw 40, from peculiarities in the monochromatic, velocity and dispersion maps.



Left Panel: H α velocity dispersion map, corrected for instrumental and thermal broadening, of the inner region of II Zw 40. The contours represent H α line intensity. The S/N_{line} of the faintest contour level is ~ 70 . Right Panel: H α radial velocity map. North is up and east is left.



Kinematics Diagnostic Diagrams (see Muñoz-Tuñón et al 1996, Yang et al 1996). I-O (left), I-V (center) and V-O (right) plots for the whole field observed in II Zw 40. Color coded pixels indicate the individual regions as shown in figure 5. Characteristic individual pixel line profiles are shown in different insets. Dashed lines represent the single Gaussian fits and the dotted line under the red profile is the instrumental profile. The vertical solid line at log(Relative Flux) = 2.5 represent our confidence level (S/N_{line} = 40). Inclined bands in the I-O (left) indicate the presence of shells in regions 3 (cyan) and 5 (black). Region 6 (magenta) seems to be unaffected by stellar evolution and that may still keep the kinematic signature of the proto-cloud that gave rise to the present starburst. It also sets a lower limit of ~ 23 kms $^{-1}$ to σ_{max} . Region 1 (red, on knot 1) seems to be kinematically very young and is dominated by random motions, not due to shells or radial velocity, likely to be associated with gravity. Results are consistent in the light of the Cometary Stirring Model of cluster formation (Tenorio-Tagle et al 1993). From V. Bordalo, H. Plana & E. Telles, ApJ, 2009, 696.1668

The brightest knot is the kinematic core

$$L \propto \sigma$$

SOME KINEMATIC CONCLUSIONS:

- The kinematic features in II Zw 40 are all remarkably similar to the ones found in supersonic GHIIRs in irregular and other star forming galaxies, powered by massive star and stellar cluster formation and evolution.
- The diagnostic diagrams of I versus σ , I versus V, and additionally σ versus V are powerful tools to identify the sources of internal motions such as shells, filaments or outflows from the presence of stellar driven winds and/or SN. These allow the de-convolution of the motions due to massive star evolution with the underlying turbulent global motions.
- The single Gaussian fit to the narrow component of an integrated emission line which encompasses the brightest knot will always measure the core line width dominated by random motions (Telles, Muñoz-Tuñón & Tenorio-Tagle 2001). This core supersonic σ is the one producing the Luminosity- σ relation (Melnick et al 1988) observed in GIIIRs and HII galaxies, and it is likely to be due mostly to gravity.
- However, we must further investigate how these derived motions precisely relate to the underlying mass distribution before we can derive absolute total galactic masses. We must also investigate, with a statistically significant sample, the possible evolutionary effects of the starburst on the observed Luminosity- σ relation and how they can be parametrized for the use as a powerful extragalactic distance estimator applied to high redshifts.
- The present application of the L- σ relation is a factor of 2 worse in errors as compared to SNe Ia in constraining cosmological parameters in the (Ω_m, w_0) plane. Terlevich et al (2015) estimate that between 100 and 300 high-z HIIIG are needed to obtain a reduction in the errors that allow similar results to the historical campaign of the present SNe Ia.
- In any case, the comparison between the SNe Ia and HII galaxy methods give us a chance of learning about the systematics affecting their accuracies, as well as teaching us about their intrinsic properties.

What's the origin of supersonic motions?

Validity to high redshift
Cosmological Distance Indicator
Hubble Diagram

$$\text{Size} \propto \sigma^2$$

$$L(\text{H}\beta) \propto \sigma^4$$

FP (O/H, W(H β), Σ_{SB})

Microphysics of SF
GMC
density, temperature, pressure

The origin of supersonic motions

- range of σ
- $\sigma_{\text{min}} - \sigma_{\text{max}}$
- Gravity
- Shells? SN, Winds

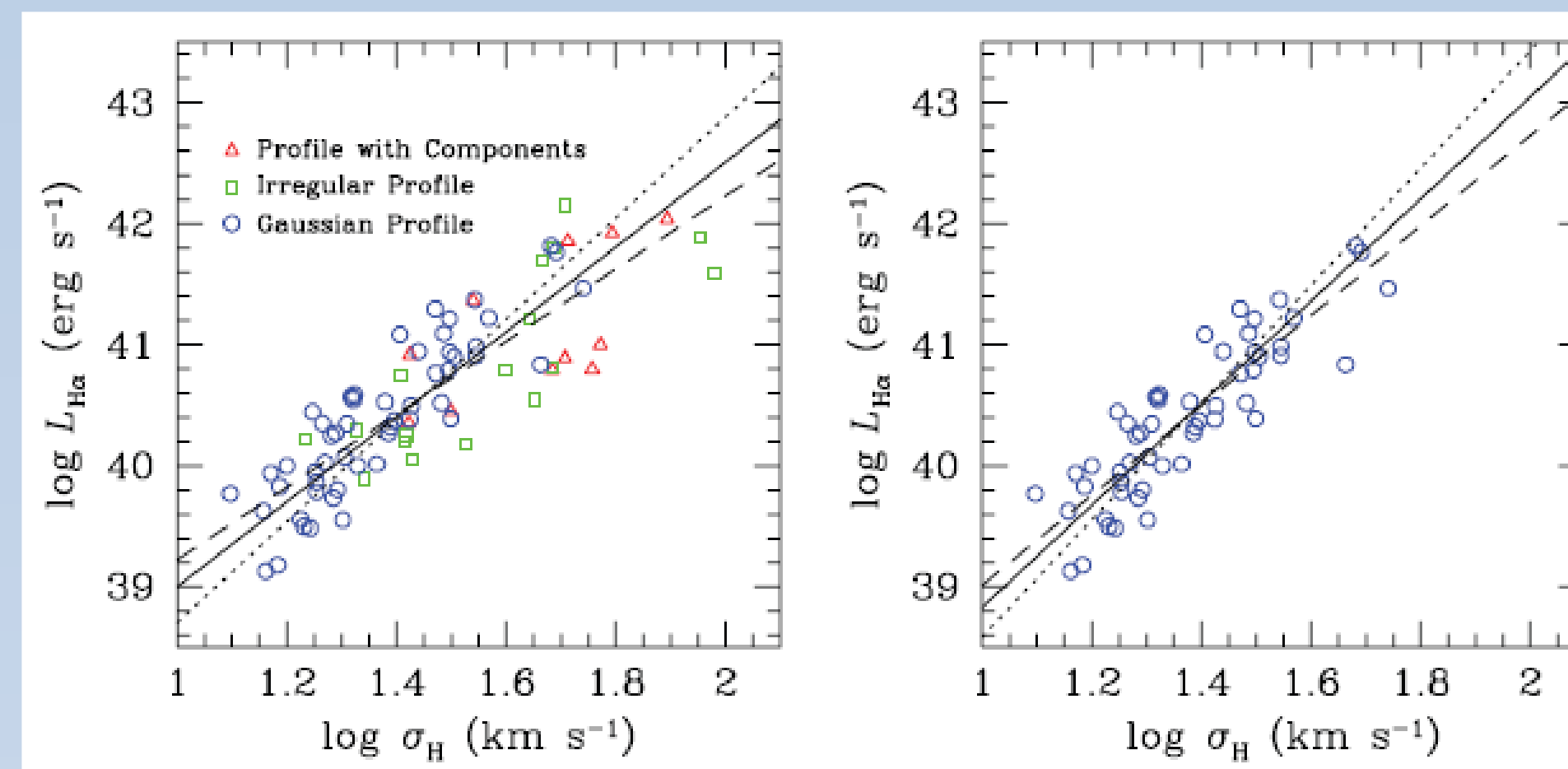
Aperture effects
Systematic effects
 L_{UBVRIJK}

Line profiles:

- Gaussian
- Irregular
- Asymmetric

M/L of starbursts
Infalling gas
Turbulence, Rotation
Outflows
Dust extinction
Calibration of emission lines
application to High redshift galaxies (galaxy families)

THE L- σ RELATION OF LOCAL HII GALAXIES



Parameters	Regressions for log L _{Hα}	rms
L- σ	$(35.26 \pm 0.38) + (3.76 \pm 0.27) \log \sigma$	0.270
L- σ -O/H	$(39.94 \pm 0.99) + (4.33 \pm 0.25) \log \sigma - (0.68 \pm 0.14) \log(\text{O}/\text{H})$	0.217
L- σ -W _{Hβ}	$(34.58 \pm 0.30) + (3.78 \pm 0.20) \log \sigma + (0.39 \pm 0.06) \log W_{\text{H}\beta}$	0.201
L- σ -[O III]/[O II]	$(34.64 \pm 0.30) + (4.09 \pm 0.21) \log \sigma + (0.39 \pm 0.07) \log([\text{O III}]/[\text{O II}])$	0.204
L- σ -O/H-W _{Hβ}	$(36.64 \pm 1.38) + (4.01 \pm 0.25) \log \sigma - (0.27 \pm 0.18) \log(\text{O}/\text{H}) + (0.29 \pm 0.09) \log W_{\text{H}\beta}$	0.197
L- σ -O/H-[O III]/[O II]	$(37.04 \pm 1.29) + (4.26 \pm 0.22) \log \sigma - (0.32 \pm 0.17) \log(\text{O}/\text{H}) + (0.28 \pm 0.09) \log([\text{O III}]/[\text{O II}])$	0.198

Top Figures: L(H α - σ) relation for all galaxies with homogeneous spectrophotometry (81 objects G, I, and C, left) and for only those showing regular Gaussian profiles (53 objects G, right). Table: Multiple Regressions for LHa, σ H, O/H, W_{H β} , and [OIII]/[OII]. From V. Bordalo and E. Telles, ApJ, 2011, 735:52

COSMOLOGY WITH HII GALAXIES

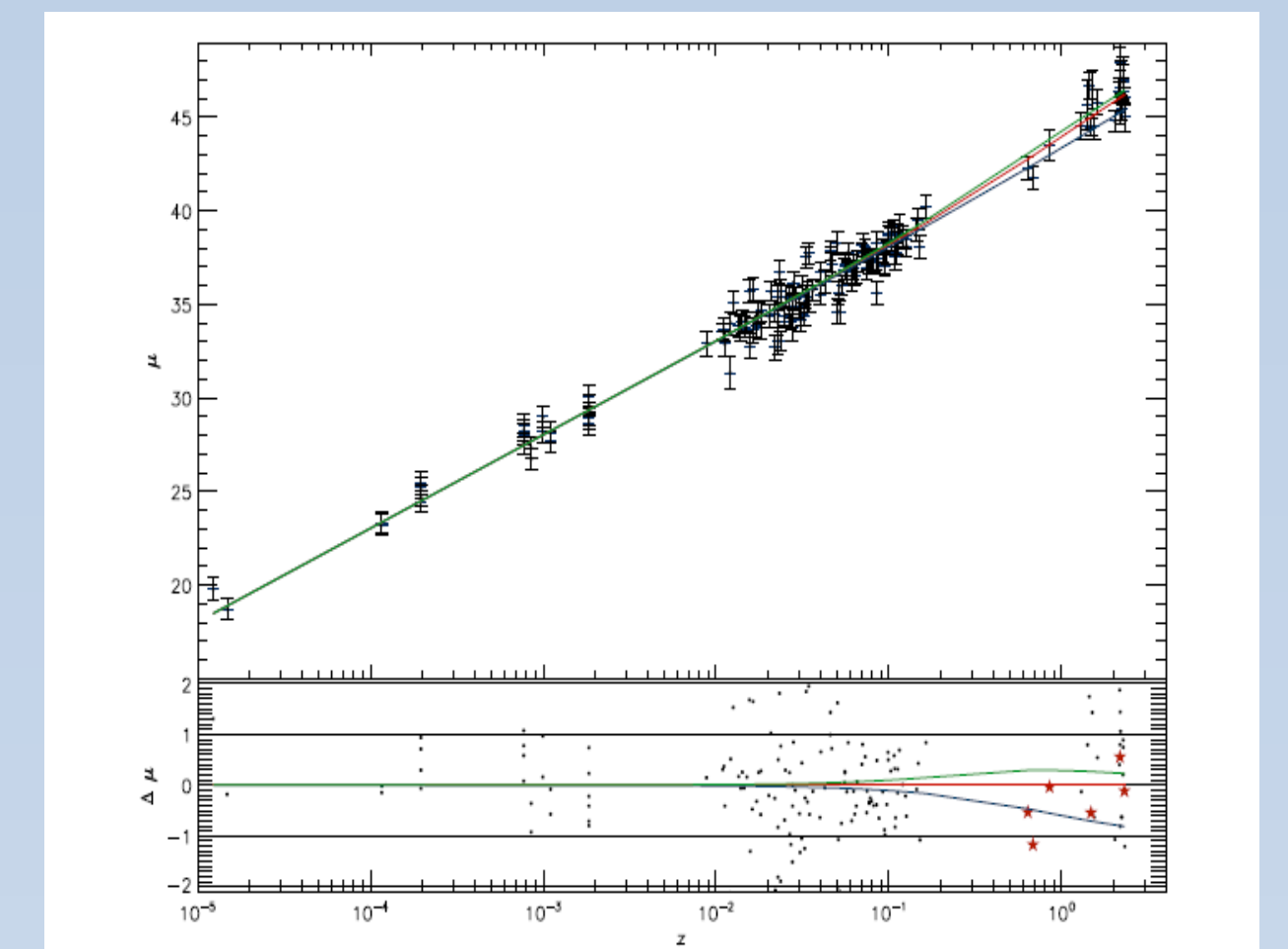
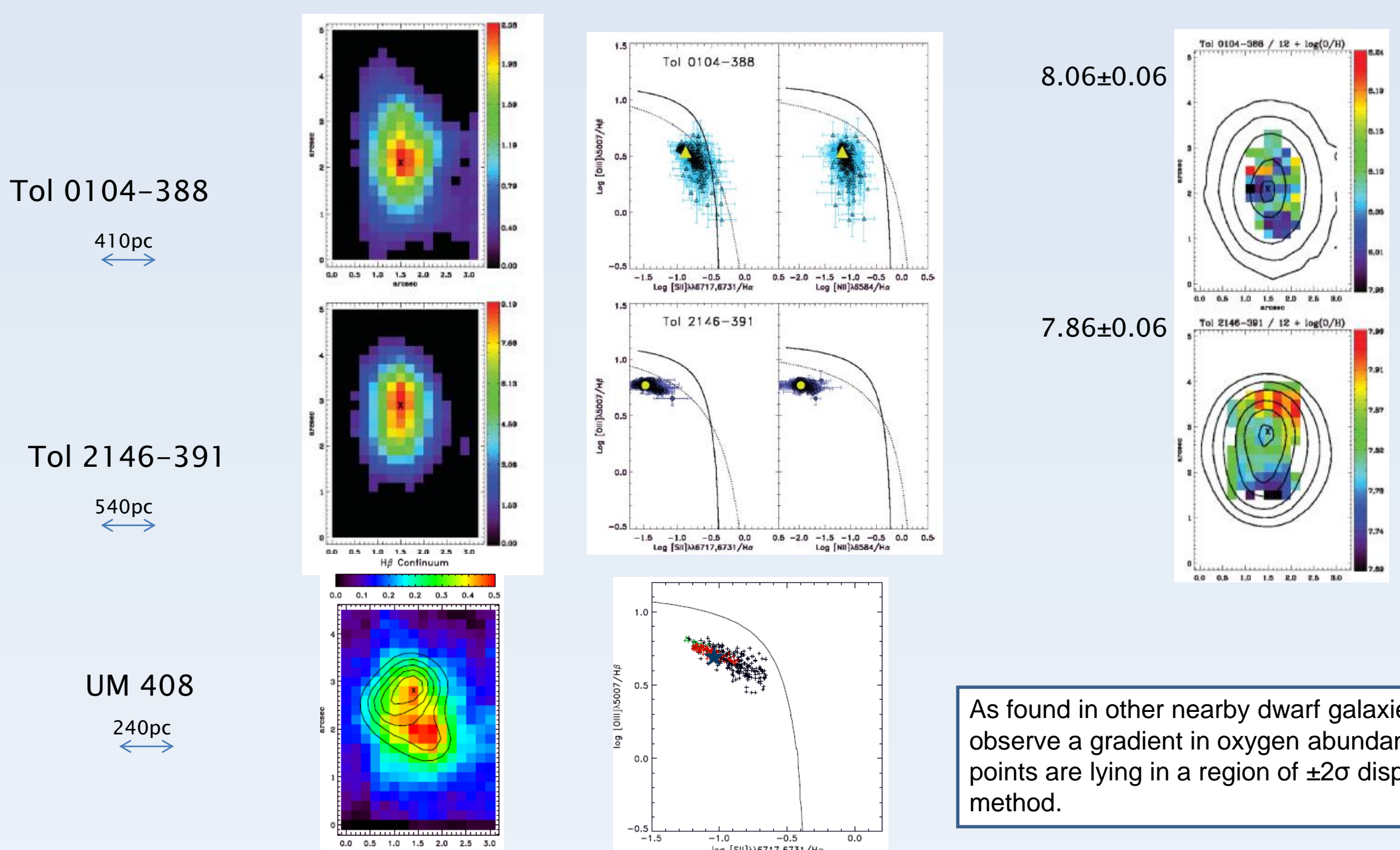


Figure 3. Hubble diagram for our sample of low and high-z HIIIG for three different cosmologies. The solid red line indicates the conventional Λ CDM cosmology with $\Omega_m = 0.3$, $\Omega_b = 0.04$, $w_0 = -1$ and $H_0 = 70$. The solid green line shows a cosmology with $\Omega_m = 0.3$ and $w_0 = -2$. The solid blue line corresponds to $\Omega_m = 0.3$ and $w_0 = 0.5$. In all three cases $\Omega_b = 0.04$ and $H_0 = 70$. The dashed lines represent the 1- σ confidence interval. The data points are color-coded according to their redshift. From Terlevich et al., 2015, MNRAS, 451, 3001

In Terlevich, R., Terlevich, E.; Melnick, J., Chávez, R.; Plionis, M.; Bresolin, F.; Basilakos, S. 2015, MNRAS, 451, 3001, the authors apply the L(H β)- σ relation for a sample of low and high redshift HII galaxies. As it has been discussed also elsewhere in a number of previous works (see references therein), the very fact of the existence of this empirical relation allows its use as a distance indicator with the cosmological interest, despite the knowledge of the origin of the internal supersonic motions (σ).

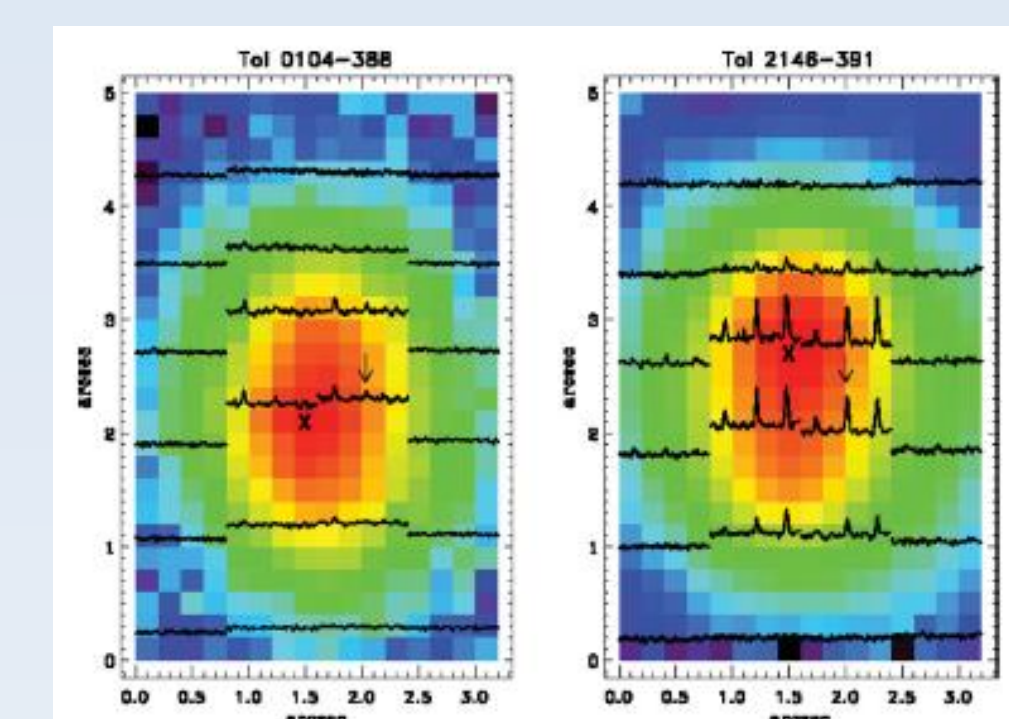
Distribution of Physical Conditions

The low and uniform metal abundances



As found in other nearby dwarf galaxies, we (Lagos et al, 2009, 2012, see poster by Lagos) do not observe a gradient in oxygen abundance across our sample galaxies. The bulk of the observed data points are lying in a region of $\pm 2\sigma$ dispersion ($\sigma = 0.1$ dex). The O/H abundances are derived via Te-method.

Sources of the nebular He II λ 4686 emission line and their spatial distribution



Spatial distributions of the binned 0.8 arcsec spectra (GEMINI GMOS-IFU) in the region that contains He II λ 4686 emission line in Tol 0104-388 and Tol 2146-391. In Lagos, Telles, Nigoche-Netro & Carrasco (2012) we have shown that Tol 2146-391 with a lower metallicity has more prominent narrow lines of He II λ 4686. Given the spatial distribution of HeII λ 4686 emission in our two analysed galaxies, this high-ionizing radiation is likely associated with a radiative shocks from mix of sources, where WR stars, high mass X-ray binaries (HMXB) and O stars cannot be excluded, particularly at low metallicities.

SOME CONCLUSIONS ON METALLICITY

- the new metals formed in the current star formation episodes are not observed and reside probably in the hot gas phase ($T \sim 10$ K) (Tenorio-Tagle 1996), whereas the metals from previous star formation events are well mixed and homogeneously distributed through the whole extent of the galaxy.
- It is then plausible that the young massive clusters responsible for the ionization of the ISM have nothing to do with the currently observed metallicity of the HII galaxies. The bimodal hydrodynamic solution of a massive cluster evolution seems to support this scenario where only a small fraction of the produced metals are expected to mix with the ISM (Silich et al. 2004, Tenorio-Tagle et al. 2007, Wunsch et al. 2008, ...).

REFERENCES:

- Lagos, P., Telles, E., Muñoz-Tuñón, Carrasco, Cuisinier & Tenorio-Tagle, 2009, AJ, 137, 5068
Lagos, P., Telles, E., Nigoche-Netro & Carrasco, 2012, MNRAS, 427, 740
Melnick, J., Terlevich, R. & Moles, M., MNRAS, 1988, 235, 297
Muñoz-Tuñón, C., Tenorio-Tagle, G., Castañeda, H. O., & Terlevich, R. 1996, AJ, 112, 1636
Silich, S., Tenorio-Tagle G. & Rodríguez González, A. 2004, ApJ, 610, 226
Telles, Muñoz-Tuñón & Tenorio-Tagle 2001, ApJ, 548, 671
Tenorio-Tagle, G., Muñoz-Tuñón, C. & Cox, D.P., 1993, ApJ, 418, 767
Tenorio-Tagle, G., Wunsch, R., Silich, S. & Palous, J. 2007, ApJ, 658, 1196
Tenorio-Tagle, G. 1996, AJ, 111, 1641
Wunsch, R., Tenorio-Tagle, G., Palous, J., & Silich, S. 2008, ApJ, 683, 683
Yang, H., Chu, Y.-H., Skillman, E. D., & Terlevich, R. 1996, AJ, 112, 146